Flexural Behaviour and Environmental Impact of African Fan Palm Reinforced Concrete Beams under Symmetrical Loading Conditions.

Abstract

The paper presents the results of investigation on reinforced beams adopting eco-friendlymaterials for sustainable concrete. The use of African fan palm is explored to mitigate the environmental impact aimed at reducing carbon emissions associated with the production and use of steel reinforcement.The beamswere tested under a four -point loading system with the ends simply supported. The test comprised twenty-three beams that were reinforced with African fan palm bars whilst two beams were reinforced with mild steel bars to serve as control beams. The study investigated the flexural strength and deformation characteristics of the beams under monotonic loading. Two concrete strengths of 15.34N/mm^2 or 22.37N/mm^2 were adopted and proposed optimal tensile ratios for an under reinforced fan palm section. The parameters considered included the tensionbars ratio (ρ), concrete compressive strength, span-to-effective-depth ratio and loading conditions. A linear elastic behaviour of both fan palm and steel reinforced concrete beams was observed to the point of first crack load beyond which the beam stiffness continued to reduce until failure. A comparison of the experimental results with results of theoretical analysis of the beams revealed that a 1.22% increase in the tensile ratio of steel in the control beams increased the cracking moment (M_{cr}) to 36%, while the fan palm beam of the same size and same concrete strength with a higher tensile ratio of 9.69% exhibited a lower M_{cr} of 11.86%. This shows a significant effect of reinforcing steel barson concrete cracking compared to the fan palm. The averages of experimental to theoretical failure loads of fan palm to steel were comparedwith failure loads of36.52kN to 20.19kN and 32kN to 19.78kN respectively. These results of the study based on the failure mode, and failure loads,highlights the suitability of using African fan palm as substitute reinforcingmaterial for low rise buildings.Furthermore, the study alsoproposed minimum and maximum tensile ratio of0.76% and 5.60%respectively for fan palm reinforced concrete beams based on the Indian Standard and modulus of elasticity of steel.

Key words: Fan palm reinforced beams, tensile ratio, modulus of elasticity.cracking load, failure load.

1.0 Introduction

In flexural structural concrete members, concrete's inherent weakness in tension is counteracted by inclusion of reinforcing materials. While steel bars as conventional reinforcement contribute significantly to structural integrity in balancing tension and compression loads (Prewitt, 2016), they also pose environmental challenges. Empirical evidence has pointed to the fact that the use of reinforcing steel bars is a contributing factor towards global carbon emissions due to the high demand of energy for the production of steel. The steel industry accounted for approximately 7-9% of global CO_2 emissions (World Steel Association, 2019). In addition to CO_2 emissions, steel production consumes large amounts of water estimated as 34,000gallons of water per ton of steel through the extraction and processing of iron ore, leading to concerns about water scarcity (74 Recycling fact, 2024). While steel is recyclable and saves up to approximately 80% of energy required for the production of new steel, a significant portion still ends up in landfills, contributing to environmental degradation(ASM Metal Recycling, 2018). Furthermore, the durability of steel reinforcement in concrete structures is endangered by environmental factors such as corrosion(Pandit et al., 2014; Lakshmi et al., 2024a, 2024b). Corrosion of steel rebars is a major concern in standard design and construction, particularly in coastal areas where exposure to saltwater accelerates the process. This not only compromises the structural integrity of buildings and other infrastructuralcomponents but also necessitates costly repairs and replacements, further increasing the environmental burden. These rendered the need to explore and adopt suitable alternative reinforcing materials.

The use and adoption of natural and eco-friendly reinforcement materials as substitutes for steel depend on their availability, technological advancements, preferences and most importantly, environmental considerations. According to Muteb and Hassan (2020), incorporating local materials is vital towards sustainable development in the quest to meet the Sustainable Development Goals (SDG) targets of reducing carbon footprint(Nilimaa, 2023). Sustainable eco-friendly materials minimize environmental impact and present a promising alternative to traditional synthetic reinforcements such as glass and carbon fibers, which are often associated with significant environmental impacts during their production and disposal (Girijappa et al., 2019).Furthermore, natural reinforcing materials are renewable, biodegradable and mostly locally sourced, thus reducing associated cost of production and transportation (NabiSaheb and Jog, 1999). Natural reinforcement materials primarily originate from plant-based sources such as

flax, hemp, jute, sisal, African fan palm, bamboo raffia and babadua. Moreover, natural fibers often provide additional benefits, such as local economic development and support for rural communities and can be cultivated and processed.Hemp and Sisal offer good tensile strength properties as well as the latter's durability and resistance to moisture penetration (Elfordy et al., 2008; Ali and Chouw, 2013). Other natural materials such as flax(Pickering et al., 2007), coconut fiber (Coir)(Ali et al., (2012),jute(Parveen and Sharma, 2013) and wood fibers (Savastano et al., 2003)are used as natural reinforcement materials that are less harmful to the environment. Woody materials such as bamboo have proven to have a high tensile strength, though they require treatment for moisture resistance and wood boring insects and fungal attack (Kankam et al., 1988; Amada and Untao, 2001; Adom-Asamoah et al., 2017).Moreover, concerns have been raised towards limitations with the use of bamboo as reinforcement with regard to its low ductility, durability, low bond to concrete and service life span (Kumar et al., 2021; Chanra et al., 2008). Raffia palm and babaduawere foundto exhibit good tensile strength and ductility properties as reinforcing bars in structural concrete members (Kankam, 1997;Kankam and Odum-Ewuakye, 1999&2001). Babadua reinforced concrete beams possessed high stiffness qualities for both pre and post cracking stages as well as good span-to-effective depth ratios (Kankam and Odum-Ewuakye, 1999).

In reinforced concrete design, mechanical properties such as tensile strength, compressive strength, modulus of rupture and modulus of elasticity and compression are important factors to consider when designing for serviceability limit state. Several research works conducted on the mechanical characteristics of the African fan palm reported significance progress on strength properties such as modulus of rupture, compression and modulus of elasticity(Samah et al., 2015; Kone et al., 2021; Ngargueudedjim et al., 2015; Asafu-Adjaye Osei Asibe et al., 2013;Sohounhloue et al., 2018). Audu and Raheem (2017) and Audu and Oseni (2015)investigated the crack parameters and patterns in concrete slabs reinforced with fan palm and subjected to sustained loads. The authors observed lower theoretical yield loads to experimental yielding loads ratios, which is a good indication on designing for serviceability limit state. Furthermore, they reported that increasing applied load led to increased number of cracks.Correal (2016)found the average tensile modulus of elasticity of bamboo (Guadua angustifolia bamboo) to be around 20GPaas compared to 200GPa for steelgiving a modular ratio

of 10% bamboo to steel.Kaminski et al. (2016)proposed a tensile modulus of elasticity of bamboo to be between 7.5GPa and 13GPa at 12% moisture content to give a modular ratio (steel to bamboo) between 27 and 15.38 for use indesign.Pam et al. (2001), investigated the tensile strength of fan palm and noted thatlower tensile value of reinforcement provides better warning with signs of ductility compared to higher tensile values which cause the concrete to crush without yielding. Fan palm being a natural and anisotropic material requires a higher safety factor against collapse when designing. Kankamand Odum-Ewuakye(1999) and Jimoh and Adetifa(1993) suggested a factor of safety of 2to 3 using babadua and fan palm respectively. These factors of safety are to provide adequate margin of safety measures to avoid collapse in building. Major collapsesof buildings have been attributed to materials; Oloyede et al. (2010) ranked causes of building failures in Nigeria as: (1) low quality building materials; (2) use of incompetent craftsmen, hence poor workmanship; (2) weak supervision; (4) poor building design and planning; (5) natural disaster and (6) soil type. This was also substantiated by Bikoko et al. (2019) who ranked the use of poor-quality building materials as the most common cause of building failures. The use of African fan palm as substitute reinforcement is explored in this research with the main aim of examining its behaviour under load, and the possibility of proposing limits for an under reinforced concrete beam.

2.0 Materials and Methods

The scope of the study covered flexural strength and deformation behaviour including cracking loads (P_{cr}), crack propagation, ultimate failure loads, deflections and mode of failures of these concrete reinforced members and propose optimal tensile ratios for an under reinforced fan palm section.

2.1 Materials

2.1.1 African Fan palm reinforcing bars (AFPR)

AFPR bars formed the major (almost 93%) of the main reinforcing bars used in this study with the rest 7% comprising mild steel bars in the beams. The mild steel bars consisted of 12mm diameter longitudinal main bars and 4.86mm diameter shear stirrups, both having yield strength

of 250N/mm^2. The AFPR materials were sourced mainly from fully grown African fan palm (AFP) trees. The bottom part approximately nine meters from the base of felled AFP trees were converted into quadrants. These quadrants were cut into bars of 2000mm long and square cross-sections of marketable sizes of 12mm, 16mm, 20mm, 25mm and rectangular sections of 25mm x 35mm. The pieces were stacked carefully in a carpentry workshop to air-dry for a duration of 2 months. Test specimens from the seasoned stack were weighed to determine the percentage moisture content that ranged from 11% - 13%. AFPR strips were then selected to ensure that brownish and closely dense and compacted fibre specimens were used for the test.

2.1.2 Description of Beams

Twenty-five (25) beams were cast into two different sizes of cross-sectional dimensions of 120mm width x 180mm depth and 135mm width x 235mm depth respectively and both were 2000mm length. The former had a percentage tension reinforcement range of 2.67 - 9.69 and the latter 2.78 - 6.31. Figure 1 (a) shows reinforcement cage comprising longitudinal reinforcing bars and shear stirrups for beams SB 5, 6, 11, 12, 18, 19, 23 and 24 made out of 12mm x 12mm fan palm, whilst Figure 1 (b) consists of beams SB1-SB4, SB7-SB10, SB14-SB17 and SB20-SB23 with longitudinal fan palm reinforcement and 4.86mm mild steel stirrups. The latter, SB14-SB25 were of beam size 135mm wide x 235mm deep x 2000mm long with percentage tension reinforcement ranging from 0.80 - 6.31. Equally, beams SB13 and SB25were made of 12mm steel reinforcement main bars and 4.86 mild steel stirrups. Two sets of stirrups spacing were adopted, 100mm and 130mm centres as described in Table 1. The beams were simply supported and tested after 28 days curing to determine the deflection and crack propagations and ultimate failure loads. The test beams were loaded using a UTS machine with a capacity of 2000kN.

Table 1: Description of Beams

Beam No. **Group 1**	Beam cross section (B x D) (mm)	Span-to-effective depth ratio	Stirrup type	Stirrup spacing (mm)	% tension rebar	Total % rebar	Concrete average strength (N/mm²)	Split cylinder tensile strength (N/mm²)
SB1	120 x 180	4.11	4.86 ss	100	4.22	6.92	15.34	2.22
SB2	120 x 180	4.11	4.86 ss	130	4.22	6.92	15.34	2.22
SB3	120 x 180	4.11	4.86 ss	100	4.22	8.44	15.34	2.22
SB4	120 x 180	4.11	4.86 ss	130	4.22	8.44	15.34	2.22
SB5**	120 x 180	4.11	12 fps	130	6.00	9.01	15.34	2.22
SB6**	120 x 180	4.11	12 fps	100	4.22	8.44	15.34	2.22
SB7	120 x 180	4.18	4.86 ss	100	6.70	9.44	22.37	1.83
SB8	120 x 180	4.06	4.86 ss	130	2.67	5.33	22.37	1.83
SB9	120 x 180	4.32	4.86 ss	100	9.69	14.12	22.37	1.83
SB10	120 x 180	4.32	4.86 ss	130	9.69	14.12	22.37	1.83
SB11**	120 x 180	4.32	12 fps	100	9.69	14.12	22.37	1.83
SB12**	120 x 180	4.11	12 fps	100	4.22	6.92	22.37	1.83
SB13*	120 x 180	4.22	4.86 ss	100	1.22	2.07	15.34	2.22
Group 2								
SB14	135 x 235	3.09	4.86 ss	100	4.40	7.21	15.34	2.22
SB15	135 x 235	3.09	4.86 ss	130	4.40	7.21	15.34	2.22
SB16	135 x 235	3.16	4.86 ss	100	6.31	9.19	15.34	2.22
SB17	135 x 235	3.16	4.86 ss	130	6.31	9.19	15.34	2.22
SB18**	135 x 235	3.37	12 fps	130	5.04	7.00	15.34	2.22
SB19**	135 x 235	3.05	12 fps	100	2.78	5.56	15.34	2.22
SB20	135 x 235	3.09	4.86 ss	100	4.40	8.80	22.37	1.83
SB21	135 x 235	3.16	4.86 ss	100	6.31	10.81	22.37	1.83
SB22	135 x 235	3.16	4.86 ss	130	6.31	10.81	22.37	1.83
SB23**	135 x 235	3.09	12 fps	100	4.40	7.21	22.37	1.83
SB24**	135 x 235	3.16	12 fps	130	6.31	9.19	22.37	1.83
SB25*	135 x 235	3.11	4.86 ss	100	0.80	1.60	22.37	1.83

Key: SS – steel stirrups; fps – fan palm stirrups; ** fan palm rebars and stirrups;

* Steel rebars and stirrups.

(a) Fan palm bars and stirrups (b) Fan palm bars and steel stirrups

Figure 1: Skeletal framed beams

2.1.3 Concrete

The concrete consisted of ordinary Portland cement (OPC), crushed granite as coarse aggregates of 10mm maximum size and natural pit sand. Two mix ratios were adopted to give two average strength grades as presented in Table 1. Also shown in the Table 1 is the splitting tensile strength of the concrete.

2.2 Methods

2.2.1 Tensile strength of fan palm

Six (6) samples for the tensile strength of the fan palm reinforcing bars of square cross-sectional areas of 12mm x 12mm and 20mm x 20mm were randomly selected from the stack of seasoned fan palm bars and cut to lengths of 600mm(Mansal et al., 2024). These specimens were subjected to a computerized Universal Testing Machine (UTM) with a load capacity of 2000kN in accordance with the BS EN 1008 (2002). The test specimens were gripped inside a 150mm long hollow metal bar at both ends using epoxy mixture of resin and hardener and allowed to dry for 24 hours. The epoxy resin had an excellent bond property with other materials when dried with less shrinkage. The glued metal bars enhanced the grip and prevented crushing of the fibres

of the fan palm bars during the test process, thus eliminating the tendency of premature failure leading to incorrect results. An extensometer with a 50mm gauge length was attached to the test specimen gripped into the jaws of the UTM (Fig.2a). The extensometer was then connected to the computer monitor and as load was applied, the latter automatically recorded the ultimate failure load and elongation as well as the stress versus strain curve and the Young's modulus of elasticity of the test specimen. A plot of the tensile stress-strain curve in Figure 2b shows linear relationship of the specimens with mean ultimate tensile failures and Young's modulus of elasticity of 94.67N/mm^2 and 20kN/mm^2 for the 20mm fan palm bars and 84.33N/mm^2 and 26.71kN/mm^2 for the 12mm bars respectively (Mansal et al., 2024). Similar findings were reported by Samah et al. (2015), Kone et al. (2021) and Adedeji. (2020).

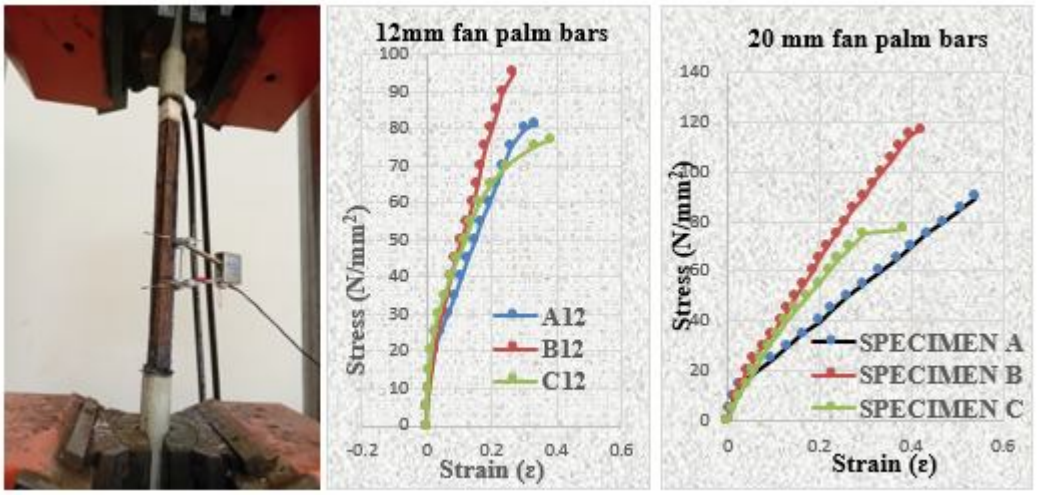

(a) Fan palm specimen (b) Stress – strain curve of the 12mm and 20mm fan palm bars

Figure 2: Tensile strength of fan palm specimens of 12mm and 20mm (Mansal et al.,2024)

2.2.2 Testing of Beams

Control beams SB13 and SB25 were reinforced with 12mm mild steel bars and 4.86 mm stirrups. The remaining beams were reinforced with fan palm bars of varied tensile ratios and with stirrups of either 4.86mm mild steel or 12mm x 12mm fan palm stirrups to resist shear. The longitudinal reinforcing bars were cut to lengths of 1950mm with shear stirrups tied at 75mm

from the inner face of the form box on both ends. Figure 3 shows a schematic diagram of the test beam. The beams were simply supported at their ends in a rigid steel frame as illustrated in Figure 4. They were incrementally loaded by means of a hydraulic jack through a rigid steel beam load spreader at 2kN intervals. The beam deflections at mid-span were recorded using a digital dial gauge at every load increment. The beams were loaded monotonically to failure.

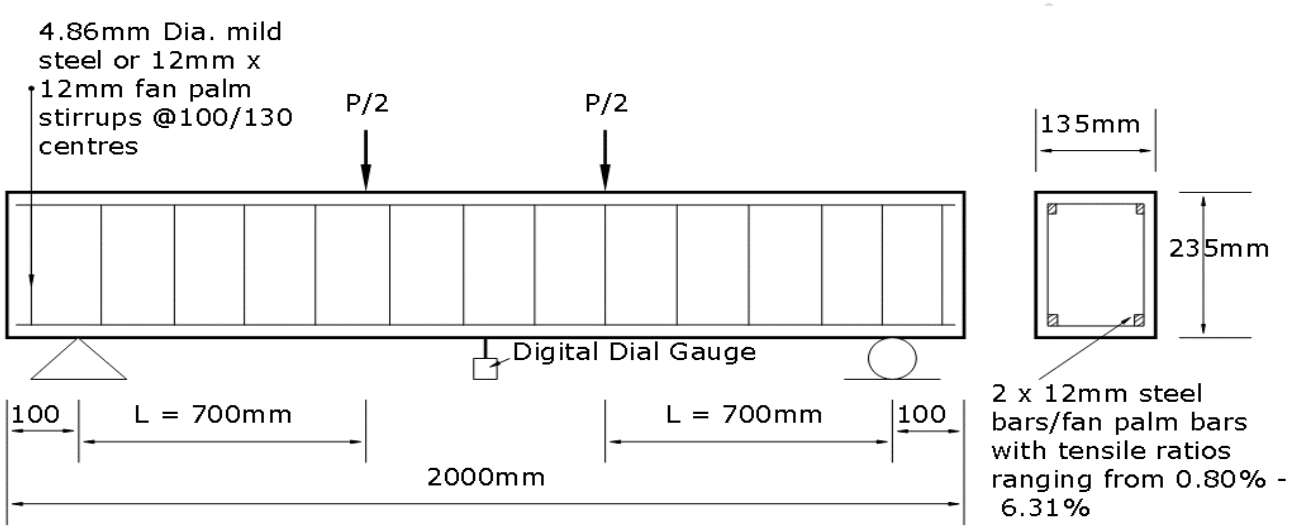

Figure 3: Schematic diagram of beam test set-up

Figure 4: Beam simply supported on a rigid frame

3.0 THEORETICAL ANALYSIS

3.1 Cracking moments and loads

3.1.1 Cracking moments

The first crack moment was estimated and computed from the split tensile strength of the concrete and the moment of inertia based on the assumption of elastic behaviour of the concrete beam at initially low applied loads prior to cracking. These two parameters are used on beams subjected to bending under relatively small loads and assuming elastic behaviour in the bending equation expressed as follows:

$$\frac{M_{cr}}{I} = \frac{f_t}{y} \quad \ldots\ldots Eq.1$$

where:

M_{cr} = cracking moment of beam; f_t = splitting tensile strength; I = second moment of area; y = distance from centreto extreme tension face (D/2); D = overall depth of beam.

From equation 1, the second moment of area of a rectangular section is computed as in Eq. 2.

$$I = \frac{BD^3}{12} \quad \ldots\ldots Eq.2$$

where:

B = width of the beam.

Hence from equations 1 and 2, the cracking moment of beam (M_{cr}):

$$Mcr = \frac{If_t}{y} \quad \ldots\ldots Eq.3$$

3.1.2 Cracking loads

An analysis of simply supported fan palm reinforced concrete beam (typically beam specimen SB1 of cross-section 120mm x 180mm and loading span of 1800mm) loaded at two-points as

shown in Figure 5 and ignoring the self-weight of the beam, gives relationship between cracking moment and cracking load as expressed in Equation 4:

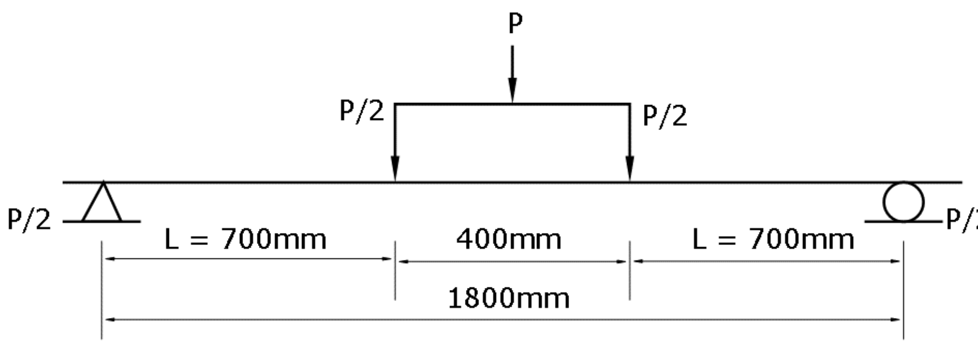

Figure 5 Simply supported fan palm reinforced beam loaded at two-points

$$M_{cr} = \frac{P_{cr}L}{2} \quad \ldots\ldots\ldots\ldots\ldots\ldots\ldots\ldots\ldots\ldots \quad Eq.4$$

where:

M_{cr} = cracking moment of the beam (kNm); P_{cr} = cracking load (kN); L = distance of support from the nearest point of load (0.7m) as in Figure 5.

Substituting to solve for P_{cr} gives Eq. 5:

$$P_{cr} = \frac{2M_{cr}}{L} \quad \ldots\ldots\ldots\ldots\ldots\ldots\ldots\ldots\ldots\ldots \quad Eq.5$$

3.2 Analysis of Theoretical Failure Load

Theoretical failure loads were assumed based on three possible scenarios, namely:

(i) reinforcing bars in tension yielding or failing first

(ii) concrete crushing first or beam failing first in compression

(iii) shear failure of beam occurring first.

3.2.1 Theoretical failure load on the assumption that the tension fan palm bars yield or fail first

The moment of resistance (M_{rs})of reinforced concrete beam on the assumption that the tension fan palm bars fail first is given by:

$M_{rs} = kf_yA_s0.775d$ Eq.6a

where $k = 1/\gamma_m$ and γ_m is the partial factor of safety of reinforcing bar; f_y = yield strength of tension bars; A_s = area of tension bars; d = effective depth. Fan pan is an anisotropic material and could exhibit different behaviour unlike steel which is homogenous and isotropic. Hence a partial factor of safety of 2.5 was assumed in the theoretical failure load to compensate for the imbalance when compared to reinforcing steel bar (γ_m = 1.15). Kankam and Odum- Ewuakye (2001) and Jimoh and Adetifa. (1991)recommended a factor of safety of 2 and 3 against collapse for babadua and fan palm, respectively. For the purpose of this study, an average factor of safety of 2.5 was used taking cue from the studies by Kankam and Odum-Ewuakye(2001) and Jimoh et al. (1991). Hence, equation 6a becomes:

$M_{rs} = 0.4f_{yp}A_{sp}0.775d$ Eq.6b

where:

f_{yp} = tensile strength of fan palm; A_{sp} = area of fan palm reinforcement in the tension zone.

The ultimate moment (M_{ultp}) of the fan palm reinforced concrete beam loaded as shown in Figure 5 is expressed in equation 7 as:

$$M_{ultp} = \frac{P_{ultp}L}{2} \quad \ldots\ldots Eq.7$$

or

$$P_{ultp} = \frac{2M_{ultp}}{L} \quad \ldots\ldots Eq.8$$

where:

M_{ultp} = ultimate moment of beam based on failure of fan palm (kNm); P_{ultp} = ultimate failure load of fan palm (kN); L = distance of support from the nearest point load (0.7m) as in Fig. 5.

Hence the failure or collapse loads of the beams based on criterion 1 (that is fan palm yielding first) is expressed by equation 8.

3.2.2 Theoretical failure load on the assumption that concrete crushes first (or beam first fails in compression)

The moment of resistance of the reinforced concrete beam, based on the assumption that the concrete crushes first in compression, including the resistance of the fan palm in compression zone is given in equation 9:

$M_{rc} = 0.156f_{cu}\, bd^2 + 0.4f_{yp}A_{sp}(d\text{-}d^{'})$ Eq.9a

In the case of beams reinforced with steel bars in both tension and compression, the equation is

$M_{rc} = 0.156f_{cu}\, bd^2 + 0.67f_{y}A_{s}(d\text{-}d^{'})$ Eq.9b

where:

M_{rc} = moment of resistance based on concrete failure in compression plus resistance of fan palmin compression; f_{cu} =concrete compressive strength; b = width beam, d = effective depth of beam; d' = depth of compression fan palm bar (i.e. inset of bar); f_{yp}= compressive strength of fan palm bars and A_{sp} = area of the fan palm bars in compression; A_s of steel stirrups; and f_y = steel strength.

Hence the ultimate failure load based on concrete crushing first is expressed in equation 10 as:

$$P_{ultp} = \frac{2M_{cr}}{L} \quad \ldots\ldots Eq.10$$

3.2.3 Theoretical failure load on the assumption that shear failure occurs first

Generally, shear failure is a combination of the action of shear and normal stresses through the formation of diagonal cracks. The resultant failure is due mostly when shear stresses within the beam exceed the material's shear capacity. Shear failure sometimes occurs with little warning and should be checked in ultimate limit state design. ACI Committee 318-14, provides guidelines and formulas to ensure sufficient shear capacity. In accordance with BS 8110-1 (1997); the shear failure load (V_r) including resistance of steel bars as stirrups in the beam is given as:

$$V_r = 0.87\frac{A_{sv}}{S_v} f_{yv}\, d + v_c bd \quad \ldots\ldots Eq.11a$$

where:

V_r= shear failure load; v_c = design concrete shear strength; f_{yv} = yield strength steel stirrups in beam SB1; A_{sv} = cross-section area of the links at the section of the neutral axis.

S_v = spacing of the links along beam SB1; B = width of the beam; d = effective depth of beam.

While adopting equation 11(a) for fan palm stirrups, equation 11(a) modifies to equation 11(b) to give:

$$V_r = 0.4\frac{A_{sv}}{S_v} f_{yp}\, d + v_c \text{bd} \quad \text{Eq. 11b}$$

where:

f_{yp} = strength of the fan palm stirrups. A factor of safety of γ_m = 2.5 is used.

The value of V_c. is obtained British Standard (BS) 8110-1-1997.

Therefore, the maximum shear force on a simply supported beam loaded at third-points is given by:

$$V_r = \frac{P_{max}}{2} \quad Eq. 12$$

or

$$P_{max} = 2V_r \quad Eq. 13$$

3.2.4 Determining fan palm tensile ratio (ρ) of reinforcement in beams

Standards and specifications are an important dimension in controlling homogeneousness of materials to guide end users. Codes of reinforcement for concrete offer insight into grades, sizes, tensile strength properties, compressive strength, yield strength for reinforced concrete structural work. Standards in Ghana relied on GS 788-2:2018,the BritishStandardonBS 4449-2005,American Standard onASTM A615and the Indian Standard onISO 6935-2:2019 for designing reinforced concrete. The BS 8110 Part 1:1997 together with the IS 456:2000 outlined the minimum percentage limit for high yield and mild steel as 0.13HYS or 0.24MS respectively, and 4 as maximum limit for both. Based on these limits, the tensile strength behaviour of the African fan palm with a factor of safety of 2.5 was used to compute for the tensile limits of fan palm. Using IS 456:2000, Clause 26.5.1.1 (a) and (b)gives the minimum tensile limits of steel ratios for the beam as:

$$(A_{sv})\text{min.} = \frac{0.85bD}{f_y} \quad \ldots\ldots Eq.14$$

and the maximum area of tension reinforcement not to exceed:

(A_{sv})max. = 0.04bD……...Eq.15

where:

A_{sv} = area of steel; b = width of the concrete beam; D = gross depth of the beam, f_y = characteristic tensile strength of steel reinforcement.

With fan palm substituted as reinforcements, and using a factor of safety of 2.5, the minimum and maximum tension reinforcement equations become:

$$(\rho)\text{min.} = \frac{0.85bD}{f_y} + \frac{0.4bD}{f_{yp}} \quad \ldots\ldots Eq.16$$

and

(A_{sv})max. = 0.04bD + 0.4bD……..…… Eq.17

Based on the Indian code, the limits that govern the adequacy of tension reinforcement when using fan palm are found to be 0.76% - 5.60%. Archila et al. (2018) compared the design strengths of steel and bamboo, based on the nominal tensile capacity, and proposes for the use of more bamboo in tension zones. Pam et al. (2000) and Archila et al. (2018)alsoexamined the contributions of tensile steel reinforced concrete with yielding and ductile failure manner (under reinforced) and tensile reinforced concrete with crushing and brittle failure effect ("over-reinforced") without yielding. The latter mode of failure and the risk of the loss of life, warrant designs to be under reinforced. Based on the observed experimental results and the Indian Code, the yielding failure mode of the beams are shown in Table 2. From Table 2, beam specimens SB5, SB7, SB9, SB10, SB11, SB16, SB17, SB21, SB22 and SB24 are all over reinforced. Amongst these specimens, SB9, SB10 and SB11 showed a 73% over reinforced beams followed by specimens SB7 with a 20%and SB16, SB17, SB21, SB22 and SB24 with a slightly 13% over reinforced sections. Beam SB5 produced a 7% over reinforced section fan palm tension reinforcing bars, with all the remaining beamswithin the serviceability limit state of under reinforced sections.

Table 2: Proposed Limits for fan palm reinforcing bars

Beam ID	Experimental failure load (kN)	Theoretical failure load (kN)	Designed of tension bar %	Max. or tensile limit %	Ratio of design and max % tensile limit	Remarks
SB1	**32**	**10.26**	4.22	5.60	0.75	Under reinforced
SB2	**30**	**10.26**	4.22	5.60	0.75	Under reinforced
SB3	**32**	**10.26**	4.22	5.60	0.75	Under reinforced
SB4	**36**	**10.26**	4.22	5.60	0.75	Under reinforced
SB5	**26**	**12.17**	6.00	5.60	1.07	*Under reinforced
SB6	**28**	**10.26**	4.22	5.60	0.75	Under reinforced
SB7	**24**	**16.30**	6.70	5.60	1.20	*Over reinforced
SB8	**16**	**6.86**	2.67	5.60	0.48	Under reinforced
SB9	**24**	**22.09**	9.69	5.60	1.73	*Over reinforced
SB10	**26**	**22.09**	9.69	5.60	1.73	*Over reinforced
SB11	**26**	**22.09**	9.69	5.60	1.73	*Over reinforced
SB12	**18**	**10.61**	4.22	5.60	0.75	Under reinforced
SB13	**38**	**16.78**	1.22	4.00	0.31	Under reinforced
SB14	**50**	**22.06**	4.40	5.60	0.79	Under reinforced
SB15	**74**	**22.06**	4.40	5.60	0.79	Under reinforced
SB16	**48**	**30.15**	6.31	5.60	1.13	*Over reinforced
SB17	**54**	**30.15**	6.31	5.60	1.13	*Over reinforced
SB18	**36**	**21.23**	5.04	5.60	0.90	Under reinforced
SB19	**22**	**14.29**	2.78	5.60	0.50	Under reinforced
SB20	**40**	**22.06**	4.40	5.60	0.79	Under reinforced
SB21	**38**	**30.15**	6.31	5.60	1.13	*Over reinforced
SB22	**40**	**30.15**	6.31	5.60	1.13	*Over reinforced
SB23	**34**	**22.06**	4.40	5.60	0.79	Under reinforced
SB24	**32**	**30.15**	6.31	5.60	1.13	*Over reinforced
SB25	**26**	**22.77**	0.80	4.00	0.20	Under reinforced

4.0 Test Results

4.1 Load-Deflection Curves

The main objective of the study was to investigate the behaviour of concrete beams reinforced with African fan palm bars to determine and predict an under-reinforced tension reinforcement for the structural members. Other important parameters observed were the failure mode and crack propagation. The load-deflection responses of the twenty-five simply supported beams loaded to failure are presented in Figures 6. These beams were incrementally loaded at intervals of 2kN using the flexural tensile testing machine. With the aid of an attached digital dial gauge, the beam central deflections were recorded and plotted at each load increment.

Figure 6 illustrates the load-deflection curves of monotonically loaded beams of similar tensile reinforcement ratio to failure. These beams were loaded incrementally at intervals of 2kN using a UTM. The beams initially showed an approximately linear relationship of the load-deflection response up to initial cracking. Upon continued increase of the load, the number of flexural cracks also increased with an observed change of slope of the load-deflection curves until the bars yielded and failed. Beams SB1 – SB6 with similar properties of span-to-effective depth ratio of 4.11 and the same percentage tensile reinforcement of 4.22, except SB5 with tensile reinforcement of 6%, exhibited the same pattern of behaviour. Specimen SB5 was the least deflected beam (4.34mm) among this category of beams. Both beam specimens SB5 and SB6 had full fan palm longitudinal tension bars and shear stirrups, but SB6 which was under-reinforced deflected three (3) times more than beam SB5 which was over-reinforced. This may be attributed to the fact that SB5 had twice tensile reinforcement of 16mm bars (6% reinforcement) with a 20mm spaced gap, thus restricting bending deflection due to increased rigidity. Beams SB9, SB10 and SB11 which were over-reinforced with 9.69% tension bars and SB12 with 4.22% tension bars (under-reinforced), produced deflections of 21.27mm, 22.67mm, 18.69mm and 18.63mm respectively. Specimens SB11 and SB 12 in the second category of beams deflected the least and is attributed to the fan palm shear reinforcement (stirrups). The load-deformation behaviour of fan palm shows abrupt failure at ultimate load either through the failure of the fan palm reinforcement or the crushing of the concrete or through diagonal

shearing. Among these loaded beams, SB13 and SB26 which were mild steel reinforced, showed larger deflections of 23.03mm and 15.23mm respectively. The fan palm reinforced beams, SB19 with a 2.78% tensile reinforcement and a span-to-effective depth ratio (a/d) of 3.05 deflected more by 11.24% compared to SB18 with a greater tension reinforcement of 5.04% and a/d ratio of 3.37. For the category of SB22 to SB25, it was observed that the deflections increased as the span-to-effective depth ratio (a/d) ratio increased. The opposite was however, observed with the same category of beams that the shear strength decreased as span-to-effective depth ratio increased.

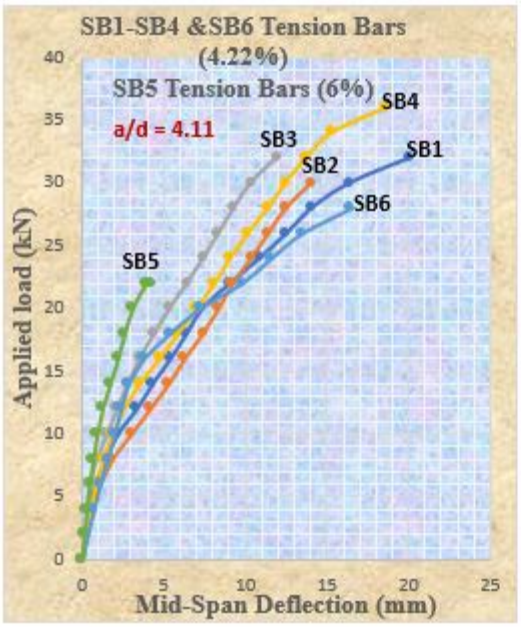
SB1-SB4 &SB6 Tension Bars
(4.22%)
SB5 Tension Bars (6%)
a/d = 4.11
SB4
SB3
SB2
SB1
SB6
SB5
Applied load (kN)
Mid-Span Deflection (mm)

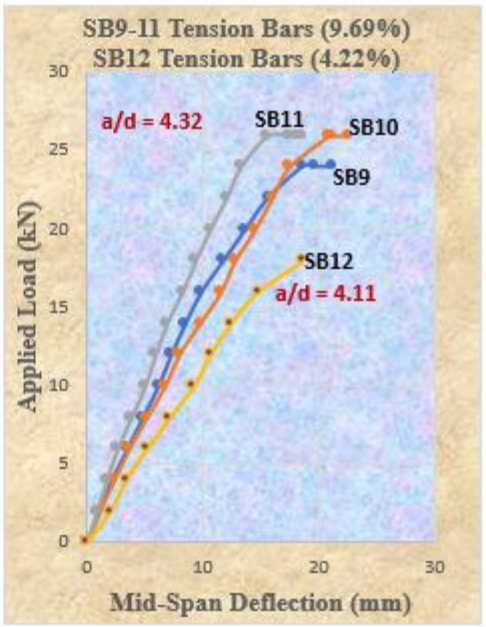
SB9-11 Tension Bars (9.69%)
SB12 Tension Bars (4.22%)
a/d = 4.32
SB11
SB10
SB9
SB12
a/d = 4.11
Applied Load (kN)
Mid-Span Deflection (mm)

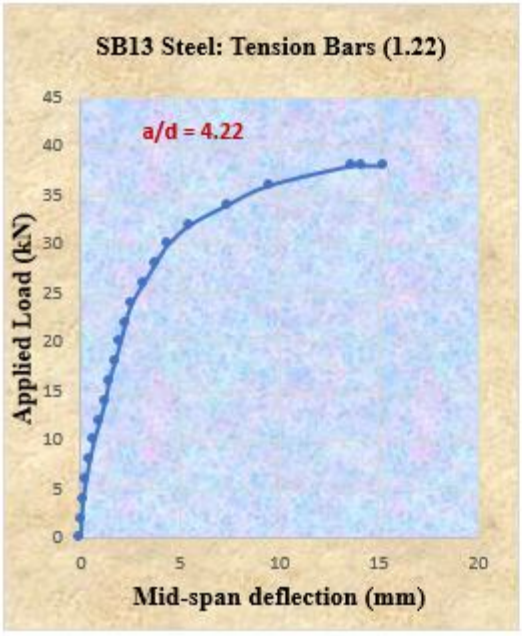
SB13 Steel: Tension Bars (1.22)
a/d = 4.22
Applied Load (kN)
Mid-span deflection (mm)

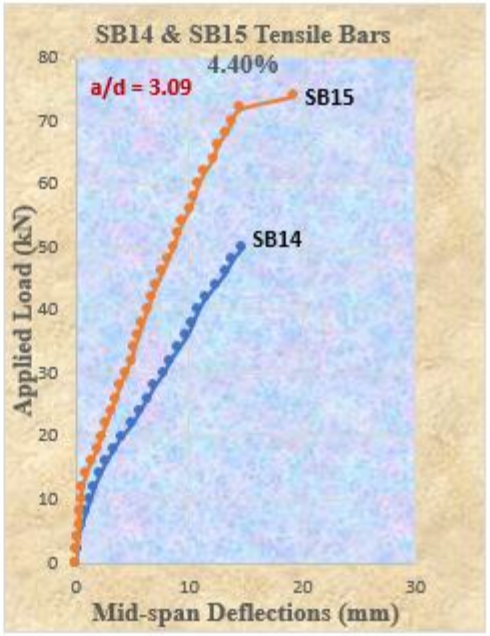
SB14 & SB15 Tensile Bars
4.40%
a/d = 3.09
SB15
SB14
Applied Load (kN)
Mid-span Deflections (mm)

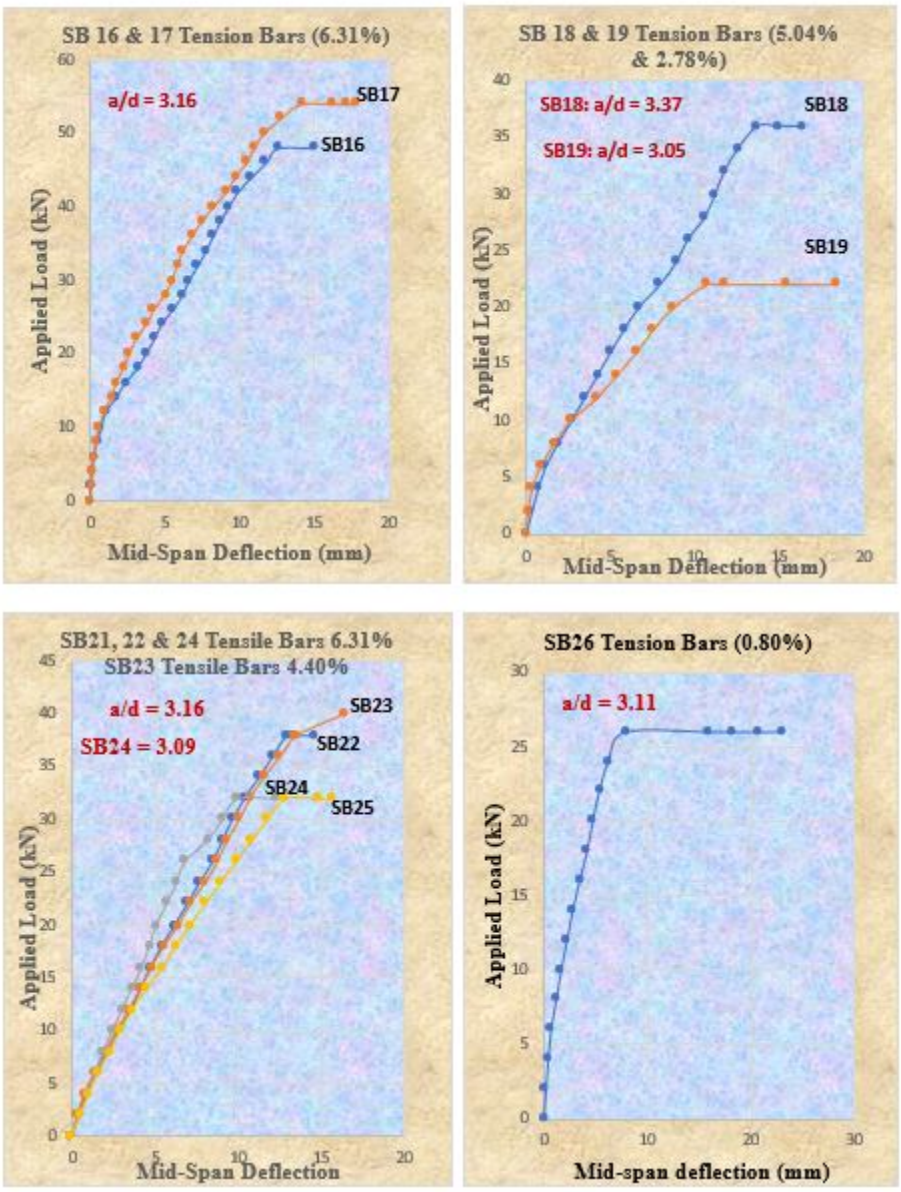

Figure 6: Load-deflection curves

4.2 Cracking Loads of Beams

The presence of numerous closely-spaced cracks formed during loading of beams indicated good bond between concrete and fan palm bars (Figure 7). Table 3 presents a comparison of the theoretical and experimental results of the cracking loads of all beams tested. The experimental cracking loads (P_{cr}) were all lower than those of the theoretical cracking loads (P'_{cr}). The ratio of theoretical cracking loads to the experimental cracking loads averaged 1.19 and 1.40 for the

120mm x 180mm and 135mm x 235mm specimens, respectively. The ratio of theoretical cracking loads to experimental cracking loads of specimens SB1-6 increased by 10.71%. A significant percentage increase was observed on the average ratio of theoretical cracking loads to experimental cracking loads of SB14 and SB15 giving an average of 44% increase.

4.3 Failure Loads of Beams

The experimental and theoretical failure loads of all specimens are presented in Table 3. Except for beams SB13 and SB25 which were reinforced with steel, all the other specimens were reinforced with fan palm bars. All theoretical failure loads were governed by failure in tension reinforcement based on a partial factor of safety (γ_m) of 2.5. Low theoretical failure loads of 10.26kN were observed for specimens SB1, SB2, SB3, SB4 and SB6 compared to experimental failure loads of (32kN, 30kN, 32kN, 36kN and 28kN respectively). This relatively low theoretical failure loads represent beams with lower percentage tension reinforcements of 4.22. Specimen SB5 of this series, had a slightly higher theoretical failure load of 12.17kN due to ahigher tensile ratio of 6% and a ratio of theoretical failure load to its experimental failure load{ $\frac{Pult\prime}{Pult}$ } of 2.13. It was also observed that theoretical failure loads of beams reinforced with mild steel (SB13 and SB25) were governed based on the yielding of the steel reinforcement. Amongst these two beams, SB25 presented almost a ratio of theoretical failure load to experimental failure load { $\frac{Pult\prime}{Pult}$ } of 1.14compared to SB13 of 2.26. Beams SB1 – SB13 with dimensions of 120mm x 180mm had an average experimental failure load of 27.38kN compared to the average theoretical failure loads of 13.87kN. On the other hand, SB14 – SB25 with dimensions of 135mm x 235mm had an average experimental load of 40.67kNcompared with their theoretical load of 23.82kN. From beam series of SB1 – SB13, the highest experimental failure load of 38kN was observed on SB13 which was steel reinforced, followed by SB4 reinforced with fan palm with failure load of 36kN. The highest theoretical failure load of 30.15kN was observed with beams SB16, SB17, SB21, SB22, and SB24. These sets of beams had the same tension reinforcement of 6.31%. Beams SB9, SB10, and SB11 with highest tension reinforcement of 9.69% had average theoretical failure loads of 22.09kN. The lowest failure load in this series was produced by beam SB8 with an experimental failure load of 16kN, and a corresponding theoretical failure load of 6.86kN. The low theoretical failure load represents the lowest tension bar reinforcement of 2.67%. The maximum overall experimental load of 74kN was produced by

beam SB15 that had fan palm longitudinal tension bars and steel stirrups. Beams series SB1 to SB6 and SB14 and SB15 produced the highest average ratios of theoretical to experimental loads of 65.50% and 64.42% and the least observed were the series of SB9 to SB12 (18.21%) and SB21 to SB24 with 21.86%.It was observed that more additional tension fan palm bars increased the load carrying capacity of the beams and reduced ductility. Therefore, narrower strips are more ideal to thicker members. This was corroborated by Harries et al. (2007), who opined that more additional Glass Fiber Reinforced Polymer (GFRP) strengthens load carrying capacity while ductility decreases.

Table 3: Failure Loads of Beams

Beam ID	Theoretical cracking load P'cr	Experimental		Theoretical failure load P'ult (kN) Based on:			P'ult/ Prc	P'ult/ P'cr	Pcr /P'ult	Pcr / P'cr	P'ult / Pult	P'ult /P'cr
		Cracking load (Pcr)	Failure load (Pult) (kN)	Fan palm/steel bars failing in tension	Concrete failing in compression	Shear						
SB1	4.11	4.0	32	10.26*	28.11	43.08	2.57	2.50	0.13	0.97	3.20	7.79
SB2	4.11	3.0	30	10.26*	28.11	37.20	3.42	2.50	0.10	0.73	2.94	7.30
SB3	4.11	3.5	32	10.26*	32.26	43.08	2.93	2.50	0.11	0.85	3.20	7.79
SB4	4.11	4.0	36	10.26*	32.26	43.08	2.57	2.50	0.11	0.97	3.51	8.76
SB5	4.11	3.5	26	12.17*	23.31	37.08	3.48	2.96	0.13	0.85	2.13	6.33
SB6	4.11	4.0	28	10.26*	32.26	49.02	2.57	2.50	0.14	0.97	2.73	6.81
Average	**4.11**	**3.67**	**30.67**	**10.58***	**29.39**	**42.09**	**2.92**	**2.57**	**0.12**	**0.89**	**2.95**	**7.46**
SB7	3.39	2.8	24	16.30*	40.00	43.96	5.82	4.81	0.12	0.83	1.47	7.08
SB8	3.39	2.5	16	6.86*	38.37	37.30	2.74	2.02	0.16	0.74	2.33	4.72
SB9	3.39	2.8	24	22.09*	38.40	41.54	7.89	6.52	0.12	0.83	1.09	7.08
SB10	3.39	2.8	26	22.09*	38.40	35.94	7.89	6.52	0.11	0.83	1.18	7.67
SB11	3.39	3.0	26	22.09*	38.40	46.00	7.36	6.52	0.12	0.88	1.18	7.67
SB12	3.39	3.0	18	10.61*	37.40	48.34	3.54	3.13	0.17	0.88	1.70	5.31
Average	**3.39**	**2.9**	**23.50**	**19.22***	**38.15**	**42.96**	**6.67**	**5.67**	**0.13**	**0.86**	**1.49**	**6.93**
SB13	10.29	7.5	38	16.78*	29.14	45.06	2.24	1.63	0.20	**0.73**	**2.26**	3.69
SB14	10.29	5.0	50	22.06*	57.14	45.12	4.41	2.14	0.10	0.49	2.27	4.86
SB15	10.29	6.5	74	22.06*	57.14	37.28	3.39	2.14	0.09	0.63	3.35	7.19

Average	**10.29**	**5.75**	**62**	**22.06***	**57.14**	**41.2**	**3.90**	**2.14**	**0.09**	**0.56**	**2.81**	**6.03**
SB16	10.29	7.5	48	30.15*	54.00	53.78	4.02	2.93	0.16	0.73	1.59	4.66
SB17	10.29	8.5	54	30.15*	54.00	46.14	3.55	2.93	0.16	0.83	1.79	5.25
Average	**10.29**	**8.00**	**51.00**	**30.15***	**54.00**	**49.96**	**3.79**	**2.93**	**0.16**	**0.78**	**3.38**	**4.96**
SB18	10.29	6.0	36	21.23*	43.94	50.00	3.54	2.06	0.17	0.58	1.70	3.50
SB19	10.29	6.0	22	14.29*	58.40	63.22	2.38	1.39	0.27	0.58	1.54	2.14
Average	**10.29**	**6.0**	**29**	**17.76***	**51.17**	**56.61**	**2.96**	**1.73**	**0.22**	**0.58**	**1.62**	**2.82**
SB20	8.48	6.5	40	22.06*	75.97	47.60	3.39	2.60	0.16	**0.77**	**1.81**	4.72
SB21	8.48	7.5	38	30.15*	72.74	56.66	4.02	3.56	0.20	0.88	1.26	4.48
SB22	8.48	7.5	40	30.15*	72.74	49.02	4.02	3.56	0.19	0.88	1.32	4.72
SB23	8.48	5.6	34	22.06*	75.97	62.84	3.94	2.60	0.16	0.66	1.54	4.01
SB24	8.48	6.0	32	30.15*	72.74	51.08	5.03	3.56	0.19	0.71	1.06	3.77
Average	**8.48**	**6.65**	**36.0**	**28.13***	**73.55**	**54.90**	**4.26**	**3.32**	**0.19**	**0.78**	**1.28**	**4.25**
SB25	8.48	6.0	26	22.77*	78.60	56.08	3.80	2.69	0.23	**0.71**	**1.14**	3.07

***Governing theoretical failure loads**

4.4 Cracking Pattern of Beams

Table 4 presents the characteristic crack patterns and failure modes of the beams. Beams SB1-SB4 failed in tension producing more flexural-shear failure cracks than pure shear failure cracks. These four beams were made from the same characteristic strength of 15.34N/mm^2, a span- to-depth ratio of 4.11, tension bar percentage reinforcement of 4.22 and the same loading conditions. Hence, their cracking moments (M_{cr}) and theoretical cracking loads (P_{cr}) are 1.44kNm and 4.11kN respectively. These four beams had an average of 14.25 cracks per beam at failure and majority of cracks registered were pure shear and flexural. Amongst these four beams, SB1 exhibited maximum crack width of 7mm at failure. Beams SB5 and SB6 with fan palm shear reinforcement showed maximum average crack spacing of 131.11mm and 110.17mm respectively. Specimen SB5 had the lowest deflection (4.34mm) of all beams, despite its relative high tension percentage fan palm of 6. The deflection reflects the 16mm slender fan palm bar

size used with minimal tendency to resist further deflection upon additional load. Beam SB14 had the maximum crack width of 10mm with 14 cracks and flexural shear cracks extending to the compression zone of the beam. Beams SB7 and SB20 developed the largest number of cracks at 17 and 20 respectively, with the former failing through diagonal flexural tension as well as a bond failure. Similarly, BeamsSB25 reinforced with 12mm mild steel bars with a characteristic strength of 250N/mm^2 failed with a distribution of twelve cracks: four pure shear cracks within the constant moment area; four flexural cracks outside the constant moment area, and four diagonal shear cracks. All pure cracks were found to terminate mid length of the beam section. Generally, the presence of a large number of cracks is a sure sign of good bond between the fan palm and concrete. This is attributed to the rough fibrous nature of fan palm which provides a good grip to the concrete compared to other natural materials such as bamboo and babadua with smooth surfaces, except that bamboo and babadua's nodes tend to enhanceinterlock with concrete(Kankam et al., 1988; Kankam and Odum-Ewuakye, 1999).

4.5 Failure Mode of beams

Figure 7 depicts typical beams at failure which show different types of cracks. The failure mode of a beam is dependent on various factors such as bond between reinforcing materials and concrete, strength of concrete, stirrups types and spacing, dowel action of the tensile bars etc. Table 4 presents three types of failures that were observed in the beams, namely: (1) pure flexural within the constant moment zone, (2) flexural-shear and (3) diagonal shear. Beams SB7 andSB12 exhibited flexural shear and bond failure at the tensile zone of the beam. Beams SB14 and SB15 exhibited flexural shear cracks extending into the compression zone, while SB16 had concrete crushing at the compression zone. This beam had a tension bar ratio of 6.31% and a compression bar ratio of 2.88% giving it a total 9.19% total reinforcement.

Table 4: Cracking Mode of Beams

Beam ID	Max. deflection (mm)	Ave. crack spacing (mm)	Max. crack width at failure (mm)	No. of cracks at failure	Type of crack at failure			Failure Mode
					Pure shear	Flexural	Diagonal shear	
SB1	20.14	51.00	7	15	8	6	1	Flexural Shear
SB2	14.07	85.58	1.5	13	5	8	0	Flexural Shear
SB3	12.01	76.33	2	16	7	9	0	Flexural Shear
SB4	18.69	95.58	1.5	13	6	2	5	Flexural Shear
SB5	3.98	131.11	5	10	4	6	0	Flexural Shear
SB6	16.46	110.17	2.5	13	4	9	0	Flexural Shear
SB7	20.57	78.88	3	17	6	5	6	Diagonal Shear & Bond
SB8	21.00	102.85	3	13	6	7	0	Flexural Shear
SB9	21.27	73.38	2.5	16	5	4	7	Diagonal Shear
SB10	22.67	84.79	3	14	5	3	6	Diagonal Shear
SB11	18.69	92.00	4.5	15	6	4	5	Diagonal Shear
SB12	18.63	93.47	5	16	6	10	0	Diagonal Shear & Bond
SB13	15.23	80.14	3.5	14	6	8	0	Flexural Shear
SB14	14.76	84.64	10	14	8	6	0	Flexural Shear to Comp. Zone
SB15	19.30	165.71	5	7	2	2	3	Flexural Shear to Comp. Zone & Bond
SB16	16.61	108.33	5	12	4	8	0	Diagonal Shear & Conc. Crushing at top
SB17	17.83	85.50	2	16	5	3	8	Flexural Shear
SB18	16.34	100.00	2	14	7	4	3	Flexural Shear
SB19	18.41	127.00	6	11	5	6	0	Flexural Shear
SB20	18.96	88.33	4	18	8	2	8	Flexural Shear
SB21	14.55	110.00	4	9	5	4	0	Flexural Shear
SB22	16.40	114.67	7	12	6	3	3	Flexural Shear & Bond
SB23	12.27	116.79	5.5	14	6	4	4	Diagonal Shear
SB24	15.62	89.69	2	16	6	6	4	Diagonal Shear
SB25	23.03	90.31	2.5	13	5	4	4	Flexural Shear

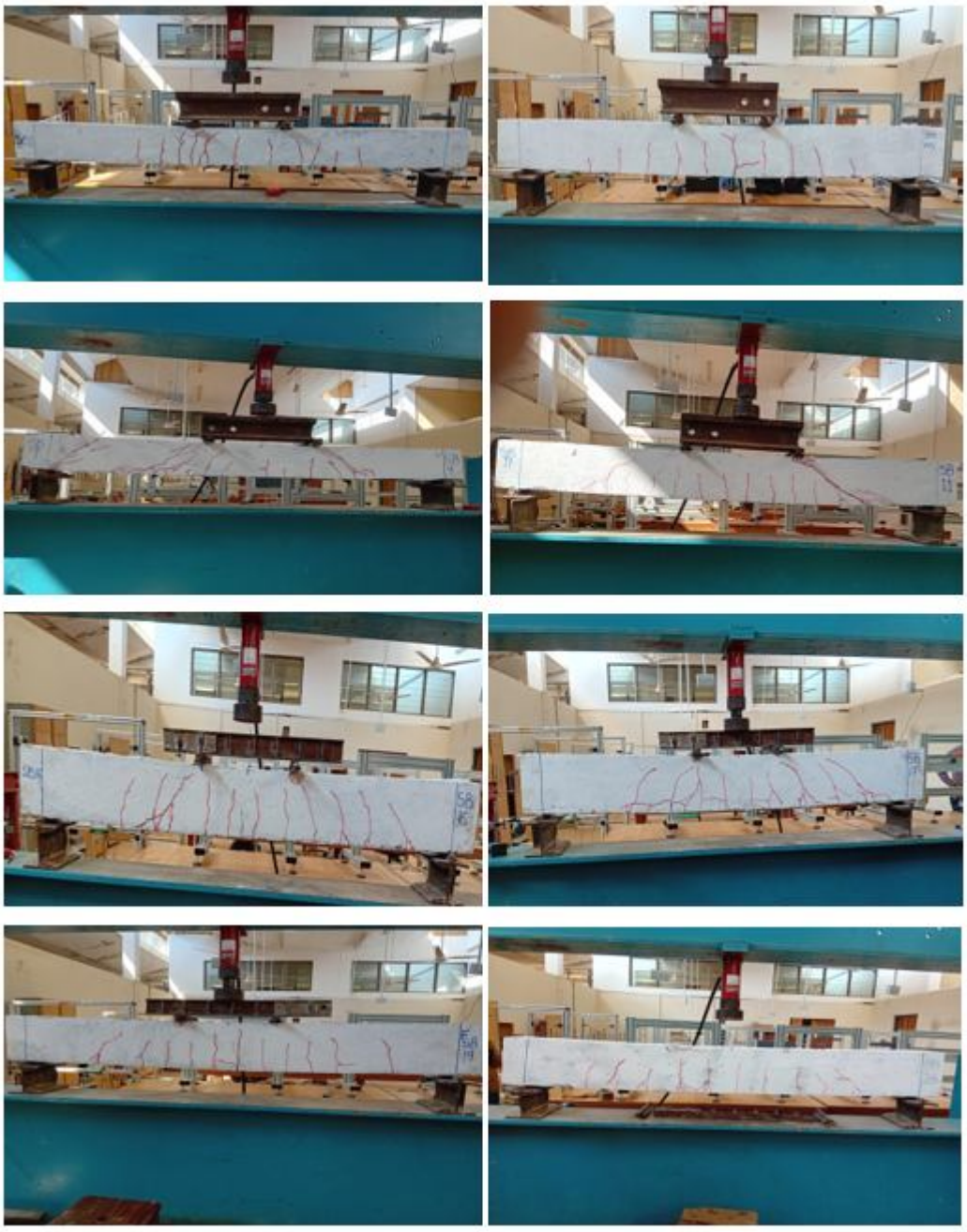

Figure 7: Crack pattern of fan palm reinforced concrete beam

5. Discussions

The load-deflection curves are presented in Fig.6. The curve showed three important points: the initiation of first cracks, indicated by the change of slope of the curve; the yielding of the tension bars and the abrupt failure at ultimate load. The failure pattern of the fan palm bars in the tensile test is similar to steel except that the yielding of the steel bar showed necking before plastic deformation and eventual failure. Maximum deflections (at failure) of the fan palm beams ranged from 3.98mm to 22.67mm.The experimental failure loads of beams with different percentage reinforcing bars were compared to the predicted theoretical failure loads.The experimental and theoretical failure loads of all beams are presented in Table 3 ranging from 16kN – 74kN and 6.86kN – 30.15kN respectively. The experimental failureloads for beams SB1-SB6 and SB7-SB12averaged2.95and 1.49 theoretical failure load respectively, thus providing a good margin of safety for theoretical analysis. Similar safety margins were observed on the rest of the beams. This in fact means that the partial factor of 2.5 adopted for the fan palm in theoretical analyses can in fact be reduced. However, the value of 2.5 was selected to accommodate the possible variabilities in the mechanical properties of fan palm across different regions. The theoretical results showed that failure loads of beams were allgoverned by bars failing first.Equally, the observed failure loads and the computation using IS 456:2000 suggested beams reinforced with fan palm tension bars above 5.6% as over-reinforced (Table 2).Table 4 underlined important characteristics of the cracking mode of beams. The presence of numerous cracks on the specimens indicated good bond between concrete and the fan pan.This is one of the key advantages of using fan palm over bamboo. Research conducted by Chanra et al., (2013) and Kumar et al., (2021) on bamboo-reinforced concrete highlighted numerous issues such as low bond and durability and brittleness.

6. Conclusions

The flexural strength and deformation properties of simply supported reinforced concrete beams with African fan palm/steel have been experimentally and theoretically studied. The study determines the suitability of African fan palm as substitute reinforcing bars based on its durability and mechanical properties such as the tensile strength and modulus of elasticity. The use of African fan palm was adopted to mitigate the environmental impact on the use of steel.Based on the results, the following conclusions are drawn:

1 Using fan palm as substitute reinforcement in concrete beams offers adequate flexural strength, but the mode of failure is abrupt. An increase in the tension bar percentage of fan palm strengthens the capacity, but reduces ductility as in the case of SB5 with double rows of tensile bars giving a ratio of 6%.

2 The load-deflection characteristics of fan palm reinforced concrete beams showed an increased tensile ratio increases the cracking load as observed in the results.

3 Fan palm beams reinforced with lower tension bars ratio showed more ductility compared to similar beams with higher tensionratio.

4 It was observed that the deflections increased as the span-to-effective depth ratio (a/d) increased. The opposite was however, observed with the same category of beams that the shear strength decreased as span-to-effective depth ratio increased.

5 Fan palm reinforced beams showed good bond between concrete and the fan palm material just like the reinforcing steel bars.

6 Based on the observed test results and using the IS 456:2000, clause 26.5.1.1 compared to the BS 8110 Part 01:1997 the tension fan palm bars ratio for an under reinforced beam section was calculated. To avoid brittle failures and provide minimal ductility, the limits that govern the adequacy of tension reinforcement using fan palm is proposed as 0.76% - 5.60%. Though it should be noted that due to the anisotropic nature of fan palm and depending on the strength of concrete used, the ratio only serves as a rule of thumb in the design of fan palm beams.

Author contribution

Contributions to the study were received from all authors.

Edward Ceasar Mansal: Conceptualization, Methodology, Validation, Analysis and Write-up.

Charles K. Kankam: Conceptualization, Methodology, Write-up - review and editing and Supervision.

Evans Biney: Experimental Investigation and Data screening.

VincentAkortia: Experimental Investigation and Data screening.

AliduBabamu: Experimental Investigation and Data screening.

Disclaimer (Artificial intelligence)

Authors hereby declare that NO generative AI technologies such as Large Language Models (ChatGPT, COPILOT, etc.) and text-to-image generators have been used during the writing or editing of this manuscript.

References

ACI Committee 318 (2014). Building Code Requirements for Structural Concrete (ACI 318-14) and Commentary (ACI 318R-14).

Adedeji RO, (2020). Determination of the utilization potentials of wood of Borassus aethiopum Mart through its strength properties. Journal of Indian Academy of Wood Science. https://doi.org/10.1007/s13196-020-00263-z.

Adom-Asamoah M, Banahene JO, and Obeng JB, (2017). Bamboo-reinforced self-compacting concrete beams for sustainable construction in rural areas. Structural Concrete - DOI: 10.1002/suco.201600205.

Ali M, and Chouw N, (2013). Coir fiber and rope reinforced concrete beam under dynamic loading. Journal of Natural Fibers, 10(1), 48-61.

Ali M, Liu A, Sou H, and Chouw N, (2012). Mechanical and dynamic properties of coconut fiber-reinforced concrete. Construction and Building Materials, 30, 814-825.

Amada S, and Untao S, (2001). Fracture properties of bamboo. Composites Part B: Engineering, 32(5), 451-459.

Archila H, Kaminski S, Trujillo D, Escamilla EZ, and Harries KA, (2018). Bamboo reinforced concrete: a critical review. Materials and Structures (2018). 51:102. http://doi.org/10.1617/s11527-018-1228-6.

Asibe AAO, Frimpong-Mensah K, and Darkwa NA, (2013). Assessment of the effect of density on mechanical properties variations of Borassus aethiopum. Archives of Applied Science Research, 5 (6); 6-19. (http://scholarsresearchlibrary.com/archive.html).

ASM Metal Recycling. (2018). The World of Metal Recycling: The Facts

ASTM A615: Standard Specification for Deformed and Plain Carbon-Steel Bars for Concrete Reinforcement; 1972.

Audu MT, and Oseni OW, (2015). First crack and Yield load of fan palm reinforced concrete Slabs. International Journal of Science and Research (IJSR). Vol. 4 Issue 11, November.

Audu MT, and Raheem AA, (2017). Flexural behavior of fan palm reinforced concrete slabs. Journal of Building Engineering. 13 (2017) 63-67.

Bikoko TGLJ, Tcamba JC, and Okonta FN, (2019). A comprehensive review of failure and collapse of buildings/structures. International Journal of Civil Engineering and Technology (IJCIET). 10(3), 2019, pp. 187 – 198.

BS 4449 (2005). Steel for the reinforcement of concrete. Weldable reinforcing steel. Bar, coil and de-coiled product. Specification. BSI.

BS 8110-1 (1997). Structural Use of Concrete, Part:1. Code of Practice for Design and Construction. London, U.K: British Standard Institution; 1997.

BS EN 1008(2002). Methods of test for water making concrete (including notes on the suitability of the water). BSI.

Chandra, Sabnani, (2013). Can Bamboo replace steel as reinforcement in concrete, for the key Structural Elements in a Low-CostHouse, Designed for Urban Poor? International Journal of Chemical, Environmental and Biological Sciences (IJCEBS). Volume 1, Issue 2. ISSN 2320-4087 (online).

Correal JF, (2016). Bamboo design and construction. In: Harries K. Sharma B (eds) Chapter 14 in nonconventional and vernacular construction materials: Characterisation, properties and applications. Woodhead (Elsevier) Publishing Series in Civil and Structural Engineering N0. 58.

Daugherty L and Cesanek J, (2024). Recycling: A Guide to Saving Energy.

Elfordy S, Lucas F, Tancret F, Scudeller Y, and Goudet L, (2008). Mechanical and thermal properties of lime and hemp concrete ('hempcrete') manufactured by production process. Construction and Building Materials, 22(10), 2116-2123.

Gana GS, Pandit P and Prashanth S, (2024). Properties of alkali activated masonry units incorporating Linz-Donawitz (LD) steel slag aggregates and Mangalore tiles waste (MTW). Materials Research Express 11 (2024) 095304. https://doi.org/101088/2053-1591/ad7812.

Girijappa YG, Rangappa SM, Parameswaranpillai V, Siengchin S (2019). Natural fibers as sustainable and renewable resource for development of Eco-friendly composites: a comprehensive review. Front. Mater, 2 p. 226, 10,3389/fmats.2019.00226. Google Scholar.

GS 788-2: 2018. Building and Construction Materials-Steel for the reinforcement of Concrete-Ribbed bars, Ghana Standard Authority; 2018.

Harries K A, Reeve B and Zorn A, (2007). "Experimental Evaluation of Factors Affecting Monotonic and Fatigue Behaviour of Fiber-Reinforced Polymer-to-Concrete Bond in Reinforced Concrete Beams," ACI Structural Journal, Nov/Dec, 2007.

International Standard ISO 6935-2:2019: Technical requirements for ribbed bars used as reinforcement in Concrete.

IS 456:2000 Clause 26.5.1.1: Plain and Reinforced Concrete – Code of Practice of India.

ISO 6935-2: (2019). Steel for reinforcement of concrete: Part 2. International Standard Publisher, Switzerland.

Jimoh Abdulahi A, and AdetifaOlajire A, Behaviour of fan-palm reinforced concrete one-way slabs subjected to flexural loading. Structural Engineering Analysis and Modelling: 27th - 29th July 1993.

Kaminski S, Lawrence A, Trujillo D, and King C, (2016). Structural use of bamboo Part 3: design values. Structural Engineering 94(12): 42-45.

Kankam CK, (1997). Raffia palm reinforced concrete beams. Journal of Material and Structures (RILEM); 30.

Kankam CK, and Odum-Ewuakye B. (1999). Structural behaviour of babadua reinforced concrete beams. Construction and Building Materials, ElsevierScience ltd., Vol 13, 187-193.

Kankam JA, Ben-George M, and Perry SH, (1998). Bamboo reinforced concrete beams subjected to third-point loading. ACI Struct J; 85(1): 61-7.

Kankam CK, and Odum-Ewuakye B, (2001). Flexural behaviour of babadua reinforced one-way slabs subjected to third-point loading. Construction and Building Material. p 27-33.

Kone O, Otieno Koteng D, Matallah M, and Kabubo CK (2021). Mechanical Characteristics of Kenyan Borassus Aethiopum Mart timber as Reinforcement for Concrete, International Journal of Civil Engineering, Vol. 8 Issue 11, pp (7-12).

Kumar P, Gautam P, Kaur S, Chaudhary M, Afreen A, and Mehta T, (2021). Bamboo as reinforcement in structural concrete.

Lakshmi A, Pandit P, Arun Kumar YM, Bhagwat Y, Nayak G, and Shetty A, (2024 a). Study on bondbehaviour of corroded reinforced concrete beams – finite element analysis. Cogent Engineering, 11(1). https://doi,org/10.1080/23311916.2024.2340298

Lakshmi A, Pandit P, Nayak G, Bhagwat Y, and Kumar S, (2024 b). Influence of corrosion-based section loss on morphology and tensile capacity of pre-stressing strands. Journal of Structural Integrity and Maintenance, 9:1, https://doi.org/10.1080/24705314. 2024. 2302655

Mansal EC, Kankam CK, Banahene JO, and Afrifa RO, (2024). Experimental investigation on the Mechanical Properties of African fan palm (Borassus Aethiopum). IOSR Journal of Mechanical and Civil Engineering (IOSR-JMCE). DOI: 10.9790/1684-2104020817. Page 8-17.

Muteb HH, and Hasan DM, (2020). Ultra-high-performance concrete using local materials and production methods. IOP Conf. Ser. Mater. Sci. Eng. 870 (1), 012100 https:// doi.org/10.1088/1757-899X/870/1/012100.

NabiSaheb D, and Jog JP, (1999). Natural Fiber Polymer Composites: A Review, Advances in Polymer Technology, Vol. 18, pp 351-363.

Ngargueudedjim K, Bassa B, Nadjitonou N, Allarabeye N, Annouar DM, Abdel –Rahim M, B.Soh Fotsing, Fogue M, JF Destrebecq, Rm Pitti, and Jerome D, (2015). Mechanical Characteristics of Tall-Palm (Borassus Aethiopum Mart., Arecaceae) of Chad / Central Africa, International Journal of Engineering and Technical Research (IJETR), Vol. 3 Issue 9, 2454-4698 (P).

Nilimaa J, (2023). Smart materials and technologies for sustainable concrete construction. Developments in the Built Environment – Elsevier, https://doi.org/10.1016/j/.dibe.2023. 100177.

Oloyede SA,Omoogun CB, and Akinjare OA, (2010). Tackling causes of Frequent Building Collapse in Nigeria. Journal of Sustainable Development. Vol. 3, No. 3, pp 127-132.

Pam HJ, Kwan AKH, and Islam MS, (2001). Flexural strength and ductility of reinforced normal – and high-strength concrete beams. Proceedings of The Institute of Civil Engineers: Structures and Buildings 2001, V. 146 n. 4, p. 381-389.

Pandit P, Venkataramana K, Babunarayan KS, Parla B and Kimura Y, (2014). "Experimental studies on the effects of corrosion on the flexural strength of RC beams," International Journal of Earth Sciences and Engineering, Vol.7, No.1 February, 2014, 320-324.

Parveen and Sharma A, (2013). Structural behaviour of jute fiber reinforced concrete beams under bending. International Journal of Engineering Research and Applications, 3(3), 108-110.

Pickering KL, Beckermann GW, Alam SN, and Foreman NJ, (2007). Optimizing industrial hemp fiber for composites. Composites Part A: Applied Science and Manufacturing, 38(2), 461-468.

Prewitt A, (2016). Acting bundling proteins and rebars structuring.

Samah OD, Amey KB and Neglo K, (2015). Determination of mechanical characteristics and reaction to fire of "Ronier" (Borassus aethiopum Mart) of Togo. African Journal of Environmental Science and Technology. Vol. 9(2), pp. 80-85. DOI: 10.5897/AJEST 2014.1767. Article Number: B79229349813. ISSN 1996-0786.

Savastano H, Warden PG, and Coutts, RSP (2003). Brazilian waste fibers as reinforcement for cement-based composites. Cement and Concrete Composites, 25(4-5), 411-419.

Sheelavantar PG, Pandit P, Prashanth S, Nishit N and Jadhav M, (2024). Taguchi-integrated grey relational analysis for multi-response optimization of mix design for alkali-activated concrete. https://doi.org/10.1088/2053-1591/ad592c.

Sohounhloue AYJ, Gbaguidi-Aisse GL, Houehanou CE and Foudjet AE, (2018). Borassus Aethiopum of Benin used as vegetable reinforcement in concrete: Characterization of the overlapping zone.

World Steel Association. (2019). "Steel's Contribution to a Low Carbon Future and Climate Resilient Societies."

74 Recycling Facts and Statistics for 2024. 10 February 2021: https://www.rts.com